Drug Design, Development and Therapy

Dovepress
open access to scientific and medical research

Open Access Full Text Article

ORIGINAL RESEARCH

Nepetoidin B Alleviates Liver Ischemia/Reperfusion Injury via Regulating MKP5 and JNK/P38 Pathway

Qiwen Yu[1], Chaopeng Mei[1], Mengwei Cui[1], Qianqian He[1], Xudong Liu[2], Xiaoxiao Du[2]

[1]Department of Emergency Medicine, the First Affiliated Hospital of Zhengzhou University, Zhengzhou, 450052, People's Republic of China; [2]Department of Hepatobiliary and Pancreatic Surgery, the First Affiliated Hospital of Zhengzhou University, Zhengzhou, 450052, People's Republic of China

Correspondence: Xiaoxiao Du, Department of Hepatobiliary and Pancreatic Surgery, the First Affiliated Hospital of Zhengzhou University, 1 Jianshe East Road, Erqi, Zhengzhou, Henan, People's Republic of China, Email xiaoxiao5811@126.com

Background: Nepetoidin B (NB) has been reported to possess anti-inflammatory, antibacterial, and antioxidant properties. However, its effects on liver ischemia/reperfusion (I/R) injury remain unclear.

Methods: In this study, a mouse liver I/R injury model and a mouse AML12 cell hypoxia reoxygenation (H/R) injury model were used to investigate the potential role of NB. Serum transaminase levels, liver necrotic area, cell viability, oxidative stress, inflammatory response, and apoptosis were evaluated to assess the effects of NB on liver I/R and cell H/R injury. Quantitative polymerase chain reaction (qPCR) and Western blotting were used to measure mRNA and protein expression levels, respectively. Molecular docking was used to predict the binding capacity of NB and mitogen-activated protein kinase phosphatase 5 (MKP5).

Results: The results showed that NB significantly reduced serum alanine aminotransferase (ALT) and aspartate aminotransferase (AST) levels, liver necrosis, oxidative stress, reactive oxygen species (ROS) content, inflammatory cytokine content and expression, inflammatory cell infiltration, and apoptosis after liver I/R and AML12 cells H/R injury. Additionally, NB inhibited the JUN protein amino-terminal kinase (JNK)/P38 pathway. Molecular docking results showed good binding between NB and MKP5 proteins, and Western blotting results showed that NB increased the protein expression of MKP5. MKP5 knockout (KO) significantly diminished the protective effects of NB against liver injury and its inhibitory effects on the JNK/P38 pathway.

Conclusion: NB exerts hepatoprotective effects against liver I/R injury by regulating the MKP5-mediated P38/JNK signaling pathway.

Keywords: liver ischemia/reperfusion injury, nepetoidin B, MKP5, JNK/P38 pathway

Introduction

Liver ischemia-reperfusion (I/R) injury often occurs during liver surgery such as liver transplantation and hepatectomy procedures.[1] In addition to directly damaging hepatocytes, liver I/R injury may affect the regenerative capacity of hepatocytes, which is an important factor affecting the success rate of liver surgery and postoperative survival.[2–4] Therefore, it is essential to develop new therapeutic methods for reducing liver I/R injury. Currently, measures to reduce I/R injury include ischemic preconditioning, drug preconditioning, and gene-targeting strategies, among which drug intervention has garnered increasing attention owing to its potential clinical application.[5–7]

Nepetoidin B (NB) is a compound derived from the genus Schizonepeta that belongs to the caffeic acid family.[8] The biological activities of NB possess anti-inflammatory, antioxidant, and antibacterial properties.[9] Studies have demonstrated that NB exerts its anti-inflammatory and antioxidant effects by regulating the nuclear factor-kappa B and Nrf2/HO-1 signaling pathways, and plays a regulatory role in insulin resistance and fat metabolism.[9,10] Inflammation and oxidative stress are important causes of liver I/R injury, and NB may also be involved in the regulation of inflammation and oxidative stress during liver I/R injury. To date, no studies have reported the potential role of NB in liver I/R injury.

Aberrant activation of the mitogen-activated protein kinase (MAPK) pathway is closely associated with liver I/R injury,[11] and the inhibition of this pathway significantly reduces liver I/R damage.[12] As important regulators of MAPK signaling pathways, MAPK phosphatases (MKPs) dephosphorylate JNK/P38 phosphotyrosine residues to inhibit the activation of MAPK signaling pathways.[13] MKP5, a member of the MKP family, inhibits the activation of the JNK/P38

Received: 13 February 2024
Accepted: 1 June 2024
Published: 17 June 2024

signaling pathway.[14] In RAW 264.7 macrophages, NB exerted anti-inflammatory effects by promoting the expression of MKP5.[10] Therefore, we hypothesized that NB plays a protective role in liver I/R injury by promoting MKP5 expression, thereby inhibiting the JNK/P38 signaling pathway.

In this study, we examined the potential protective effects of NB in mouse liver I/R and AML12 cells H/R injury models. These results demonstrate that NB can reduce liver injury and inhibit oxidative stress, hepatocyte apoptosis, and inflammation following liver I/R and H/R injury. Furthermore, NB treatment inhibited the phosphorylation of JNK/P38 proteins, and the protective effects of NB were related to an increase in MKP5 expression. These results suggest that NB is a promising therapeutic candidate for liver I/R injury.

Materials and Methods

Animals and Liver I/R Injury Model

Wild male C57BL/6 mice aged 6–8 weeks and weighing 20–25 g were purchased from the Zhengzhou University Experimental Animal Center. A total of 72 mice were used in this study (n = 6 per group). The mice were maintained in a pathogen-free environment with a 12-h light/dark cycle and had free access to food and water. The MKP5 KO mice were provided by Professor Liang Yinming of Xinxiang Medical University. Information on the construction of MKP5 knockout mice is provided in the Supplementary Materials and Supplementary Tables 1 and 2. NB (Catalog Number: HY-N8263, MedChemExpress, shanghai, China) was dissolved in dimethyl sulfoxide and diluted with normal saline. NB was administered to the mice by intraperitoneal injection with different doses at 200 μL per mouse one hour before I/R injury. The National Institutes of Health Guidelines for the Care and Use of Laboratory Animals were followed in all experiments. This study was approved by the Ethics Committee of the First Affiliated Hospital of Zhengzhou University (ethics approval no: 2018-KY-78, December 05, 2018).

A mouse model of liver I/R injury was established using previously reported methods.[15] Mice were anesthetized with intraperitoneal sodium pentobarbital. The mid-abdominal line was incised, and the middle and left liver lobe vessels were isolated and clamped using a non-invasive arterial clamp for 90 min to induce ischemia. The clamp was then removed to restore liver blood perfusion, and the mid-abdominal incision was closed using silk sutures. The sham-operated mice did not undergo vascular clamping, and the rest of the procedure was the same as that used for the I/R group. After reperfusion, blood and tissue samples were collected for further testing.

Measurement of Liver Function

Blood samples were collected after reperfusion, centrifuged at 3000 rpm for 5 min, and the supernatant was collected for analysis. Serum AST and ALT levels were measured according to the manufacturer's instructions (JianChen Bioengineering Institute, Nanjing, China).

Hematoxylin and Eosin Staining

Liver tissues were fixed in 10% formalin solution, embedded in paraffin, and cut into 5-μm-thick sections. Paraffin sections were deparaffinized, hydrated, and stained with hematoxylin and eosin (H&E) according to the manufacturer's instructions (Servicebio, Wuhan, China). The sections were then dehydrated, made transparent, and sealed with neutral gum solution. Finally, they were examined under a light microscope (Olympus, Tokyo, Japan) to determine the histopathological changes in the liver tissues.

Cell Culture and H/R Model

The H/R model of AML12 mouse hepatocytes was used to simulate I/R in vitro. AML12 cells were purchased from Wuhan Procell Biotechnology Co., Ltd (Wuhan, China). The cells were cultured in DMEM/F12 medium supplemented with 10% fetal bovine serum, 0.5% ITS-G + 40ng/mL dexamethasone, 1×10^5 U/mL penicillin, and 100 mg/mL streptomycin, and the culture was maintained at 37 °C in a 5% CO_2 constant temperature incubator. The H/R model of AML12 cells was established based on previously reported methods.[16] Prior to hypoxia, when the cell density reached 70–80%, the cells were washed twice with PBS and incubated in sugar-free and serum-free medium (Procell, Wuhan,

China) in a triple-gas incubator (5% CO_2, 94% N_2, and 1% O_2) for hypoxia. Hypoxia for 12 h was followed by the replacement of the medium with normal medium and incubation in an atmospheric incubator for 6 h to complete reoxygenation.

Cell Counting Kit-8 Assay

AML12 cells were seeded at a density of 5000 cells per well in a volume of 100 μL in 96-well plates and cultured in a normoxic incubator. When the cell density reached 70–80%, H/R was performed according to the experimental group. The NB group was treated with NB before the induction of hypoxia. The CCK-8 reagent (10 μL) (Beyotime, Shanghai, China) was added to each well after reoxygenation and incubated for 1 h in a normoxic incubator. Cell activity was calculated based on the absorption value at 450 nm, as determined by enzyme labeling (Thermo Fisher Scientific, Inc).

Oxidative Stress Index Detection

Liver tissues were homogenized by adding 1 mL of extraction solution per 100 mg of tissue, followed by centrifugation at 12,000 × g for 10 min. The supernatant was collected, and protein concentrations were determined using a BCA kit. Superoxide dismutase (SOD), malondialdehyde (MDA) and glutathione (GSH) levels were detected according to the manufacturer's instructions (Solarbio, Beijing, China). Dihydroethidium (DHE) staining (Beyotime, Shanghai, China) was used to detect reactive oxygen species (ROS) in liver tissues and AML12 cells. Briefly, liver tissue embedded in optimal cutting temperature compound was cut into 10-μm-thick sections, stained with DHE (10 μm/L), incubated at 37°C for 30 min in the dark, washed three times with PBS (Solarbio, Beijing, China), stained with DAPI (Beyotime, Shanghai, China) for 10 min at room temperature, and imaged using a fluorescence microscope (Olympus, Tokyo, Japan). For AML12 cells, 1 μL of 10 μM DHE staining solution was added to each 1 mL of medium after reoxygenation, incubated for 20 min, washed three times with PBS, stained with Hoechst (Beyotime, Shanghai, China) for 10 min at room temperature, and imaged using a fluorescence microscope (Olympus, Tokyo, Japan).

Enzyme-Linked Immunosorbent Assay

Blood samples were collected after reperfusion, centrifuged at 3000 rpm for 5 min, and the supernatant was collected to measure serum levels of interleukin (IL)-1β, IL-6, and tumor necrosis factor alpha (TNF-α) using enzyme-linked immunosorbent assay (ELISA), and all indices were detected in strict accordance with the manufacturer's instructions (Proteintech, Wuhan, China). Briefly, standard wells were added with different concentrations of standards, assay wells were added with 100 μL of serum into a primary antibody-coated 96-well ELISA microtiter plate, incubated for 1 h at room temperature, and washed three times. Next, 100 μL of 1:100 dilution of enzyme-labelled detection antibody was added to each well, incubated for 1 h at room temperature, and washed three times. Finally, 100 μL of tetramethylbenzidine substrate was added to the wells. The reaction was carried out for 20 min at room temperature, protected from light, and stopped using an ELISA stop solution. The optical density (OD) at 450 nm was measured on the ELISA, and the standard curve was plotted according to the absorbance value of the standard wells, and the concentration of the assay wells was calculated.

Real-Time Polymerase Chain Reaction

Total RNA was extracted from liver tissues and AML12 cells using TRIzol reagent (Solarbio, Beijing, China) according to the manufacturer's instructions. The RNA concentration was determined using a micro-UV spectrophotometer (Thermo Fisher Scientific, Inc.). RNA (1 μg) was reverse transcribed into cDNA according to the instructions of the transcription kit (vazyme, Nanjing, China), and cDNA was amplified on a real-time polymerase chain reaction instrument using the SYBR Green qPCR Mix reagent (vazyme, Nanjing, China). *Gapdh* was used as an internal control. The $2^{-\Delta\Delta CT}$ method was used for analysis. Primer sequences for *Il-1β, Il-6, Tnf-α*, and *Gapdh* are listed in Table 1.

Immunofluorescence Staining

Paraffin-embedded liver tissues were cut into 5-μm-thick sections and baked at 60 °C for 2 h, after which the sections were dewaxed with xylene and hydrated with gradient ethanol. The liver sections were repaired with 0.01 mol/L citrate

Table 1 Quantitative Polymerase Chain Reaction Primer Sequences

Primer	Primer Sequence
IL-1β F	5′-GCTTCAGGCAGGCAGTATCA-3′
IL-1β R	5′-AGTCACAGAGGATGGGCTCT-3′
IL-6 F	5′-AGAGACTTCCATCCAGTTGCC-3′
IL-6 R	5′-TCCTCTGTGAAGTCTCCTCTCC-3′
TNF-α F	5′-AGCCGATGGGTTGTACCTTG-3′
TNF-α R	5′-ATAGCAAATCGGCTGACGGT-3′
MCP-1 F	5′-ATCTGCCCTAAGGTCTTCAGC-3′
MCP-1 R	5′-AGGCATCACAGTCCGAGTCA-3′
GAPDH F	5′-CTGCCCAGAACATCATCCCT-3′
GAPDH R	5′-TACTTGGCAGGTTTCTCCAGG-3′

buffer (pH 6.0). After sealing with 10% goat serum for 1 h at room temperature, the sections were incubated overnight at 4 °C with primary antibodies against Ly6g (1:200; Servicebio, Wuhan, China) and CD11b (1:200; Servicebio, Wuhan, China). The sections were washed three times with PBS before and after the addition of the fluorescent secondary antibody (1:500, Servicebio, Wuhan, China), incubated for 30 min at room temperature, stained with DAPI for 10 min at room temperature, and finally blocked with an anti-fluorescence quencher (Servicebio, Wuhan, China). The sections were imaged using a fluorescence microscope (Olympus, Tokyo, Japan).

Terminal Deoxynucleotidyl Transferase dUTP Nick-End Labeling Staining

Paraffin-embedded liver tissue was cut into 5-μm-thick sections, followed by xylene dewaxing and gradient ethanol rehydration. Terminal deoxynucleotidyl transferase dUTP nick-end labeling (TUNEL) staining was performed using a TUNEL kit (Servicebio, Wuhan, China). After staining, the sections were washed three times with PBS for 5 min each. The nuclei were then stained with DAPI, incubated at room temperature for 10 min, washed with PBS three times for 5 min each, and finally sealed with an anti-fluorescence quenching agent. Sections were imaged using a fluorescence microscope.

Western Blot Analysis

Proteins were extracted from the liver tissue and cells using RIPA buffer containing 1% PMSF and protein phosphatase inhibitor (Solarbio, Beijing, China). The protein concentrations were determined using a BCA kit (Solarbio, Beijing, China). Proteins were separated by 10% or 12% SDS-PAGE, transferred to PVDF membranes, and blocked for 1 h with 5% skim milk. Membranes were incubated with anti-BCL-2 (1:1000; HUABIO, Hangzhou, China), anti-Cleaved caspase 3 (1:1000; CST, MA, USA), anti-BAX (1:1000; Proteintech, Wuhan, China), anti-p-JNK (1:1000; CST, MA, USA), anti-JNK (1:1000; Proteintech, Wuhan, China), anti-p-p38 (1:1000; CST, MA, USA), anti-p38 (1:1000; HUABIO, Hangzhou, China), anti-MKP5 (1:1000; Santa Cruz, CA, USA), and anti-GAPDH (1:5000; Proteintech, Wuhan, China) antibodies overnight at 4 °C. The following day, membranes were incubated with goat anti-rabbit (1:10000; Proteintech, Wuhan, China) or goat anti-mouse secondary antibody (1:10000; Proteintech, Wuhan, China) at room temperature for 1 h. After three washes with TBST, the membrane was developed using a gel imaging system (Cytiva, MA, USA) after the addition of ECL luminescent solution (NCM Biotech, Suzhou, China).

Flow Cytometry Analysis

After reoxygenation, cells were harvested by digestion with trypsin without EDTA (Beyotime, Shanghai, China), followed by centrifugation at 200 × g for 5 min. After washing twice with PBS, the cells were resuspended in 195 μL 1× annexin-binding buffer. Annexin V-FITC and PI (Beyotime, Shanghai, China) were sequentially added, incubated at room temperature for 10 min, protected from light, and analyzed using flow cytometry (BD Biosciences, USA).

Molecular Docking

The structure of the MKP5 protein (AF-Q9ESS0) was downloaded from the AlphaFold protein structure database. The ligand (NB) and protein (MKP5) required for molecular docking were prepared using the AutoDock Vina software (http://vina.scripps.edu/). For the MKP5 protein, the crystal structure was preprocessed, including the removal of hydrogenation, modification of amino acids, optimization of energies, and tuning of force field parameters, after which the low-energy conformation of the ligand structure was satisfied. Finally, the MKP5 target structure was molecularly docked to the NB drug structure using Vina within Pyrx software, and its affinity (kcal/mol) value represents the binding capacity of the two combinations. PyMOL was used for visualization and analysis, and 2D plots were visualised using the Discovery Studio 2020 Client.

Statistical Analysis

SPSS software (ver. 22.0; SPSS Inc., Chicago, IL, USA) was used to analyze the experimental data. Measurement data are expressed as mean ± standard deviation (SD). Student's *t*-test was used to compare two groups, and one-way ANOVA was used to compare multiple groups. Statistical significance was set at $P < 0.05$.

Results

Nepetoidin B Alleviates I/R-Induced Liver Injury and Cell Damage in vivo and in vitro

The concentrations of NB in mice and AML12 cells were determined through preliminary experiments, considering both the absence of toxic effects at lower concentrations and the observed significant effects of reducing liver I/R injury and enhancing cell activity after H/R injury. NB concentrations below 20 mg/kg did not induce any toxic effects on the livers of mice (Figure 1A and B). Furthermore, NB at 10, 15, and 20 mg/kg significantly reduced the serum ALT and AST levels. Notably, the 15 and 20 mg/kg concentrations exhibited greater efficacy than the 10 mg/kg concentration; however, there was no significant difference in efficacy between the 15 and 20 mg/kg concentrations (Figure 1A and B). Based on these findings, we selected 15 mg/kg NB for subsequent animal experiments. In AML12 cells cultured under normal oxygen conditions, NB concentrations <30 μM did not exhibit any toxic effects (Figure 1C). Moreover, NB increased the activity of AML12 cells after H/R injury in a concentration-dependent manner; however, there was no significant difference between the 20 and 30 μM concentrations (Figure 1D). Consequently, 20 μM of NB was selected for subsequent experiments. Moreover, HE staining revealed focal or large-area necrosis of liver cells in the I/R group, and the structure of the liver lobules was disturbed (Figure 1E). In contrast to the I/R group, the I/R+NB group exhibited a significant reduction in necrotic cell area (Figure 1E and F). Based on these animal and cellular studies, these results suggest that NB alleviated I/R-induced liver injury and H/R-induced cell damage.

Nepetoidin B Alleviates I/R-Induced Oxidation in vivo and in vitro

As shown in Figure 2A–C, MDA levels in the liver tissues were significantly higher, and SOD and GSH activities were significantly lower after I/R injury than in the sham group. However, compared to the I/R group, NB pretreatment resulted in a significant increase in SOD and GSH activities while inhibiting MDA (Figure 2A–C). The DHE staining results revealed that the levels of ROS in normal liver tissue and AML12 cells cultured under normal oxygen conditions were relatively low (Figure 2D–G). However, ROS levels significantly increased following I/R and H/R (Figure 2D–G). Notably, NB effectively inhibited ROS production after liver I/R and H/R injury in AML12 cells (Figure 2D–G). These results suggest that NB alleviated I/R-induced oxidation, both in vivo and in vitro.

Nepetoidin B Alleviates I/R-Induced Apoptosis in vivo and in vitro

After liver I/R injury, there was a significant increase in the number of TUNEL-positive cells in mouse liver tissue (Figure 3A and B), and cell apoptosis rates significantly increased after AML12 cells H/R injury (Figure 3C and D). In contrast, pretreatment with NB significantly reduced the number of TUNEL-positive cells in the liver tissue following I/R injury (Figure 3A and B) and the cell apoptosis rates after AML12 cells H/R injury (Figure 3C and D). Moreover, examination of apoptosis-related proteins indicated a significant increase in the levels of BAX and Cleaved caspase 3,

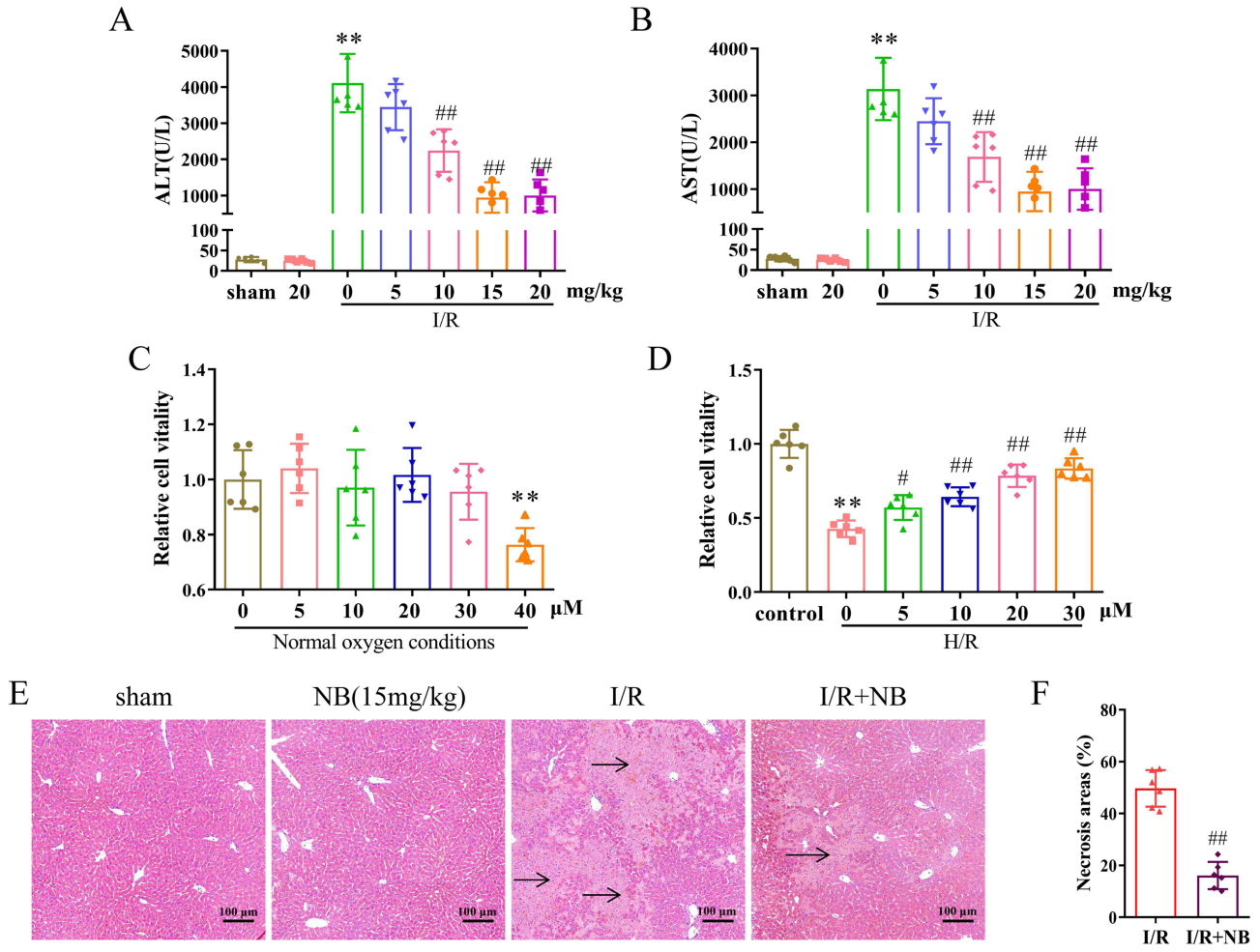

Figure 1 Nepetoidin B alleviates I/R-induced liver injury and cell damage in vivo and in vitro. (**A**) Serum ALT and (**B**) AST levels in each group (n = 6/group); (**C**) CCK8 assay was used to detect the effect of NB on the activity of AML12 cells under normal oxygen conditions (n = 6/group); (**D**) CCK8 assay was used to detect the effect of NB on the activity of AML12 cells after H/R injury (n = 6/group); (**E**) H&E staining (the area indicated by the black arrow indicates the necrotic area) and (**F**) necrotic area statistics of liver tissue in mice (n = 6/group). **P < 0.01 vs sham or control group; #P < 0.05 and ##P < 0.01 vs I/R or H/R group.

whereas there was a significant decrease in the expression of BCL-2 in the liver tissues of mice after I/R injury and in AML12 cells after H/R injury (Figure 3E–L). However, pretreatment with NB reversed these changes in the expression of apoptosis-associated proteins (Figure 3E–L). These results indicate that NB pretreatment reduced I/R-induced apoptosis both in vivo and in vitro.

Nepetoidin B Alleviates I/R-Induced Inflammation in vivo and in vitro

Following liver I/R injury, serum levels of IL-1β, IL-6, and TNF-α were significantly elevated (Figure 4A–C), whereas NB pretreatment significantly decreased the levels of IL-1β, IL-6, and TNF-α in mouse serum after liver I/R injury (Figure 4A–C). The immunofluorescence staining results indicated a significant increase in the number of $Ly6g^+$ and $CD11b^+$ cells in the liver tissues following I/R injury (Figure 4D and G), whereas the number of $Ly6g^+$ and $CD11b^+$ cells was significantly decreased in the IR+ NB group (Figure 4D–G), suggesting that NB reduced the tissue inflammatory response following liver I/R injury. Furthermore, we detected the mRNA expression of *Il-1β, Il-6*, and *Tnf-α* in AML12 cells subjected to H/R injury and found that the mRNA expression of *Il-1β, Il-6*, and *Tnf-α* was significantly increased following H/R (Figure 4H–J), whereas pretreatment with NB significantly inhibited the mRNA expression of inflammatory factors (Figure 4H–J). These results suggest that NB inhibited I/R-induced inflammation both in vivo and in vitro.

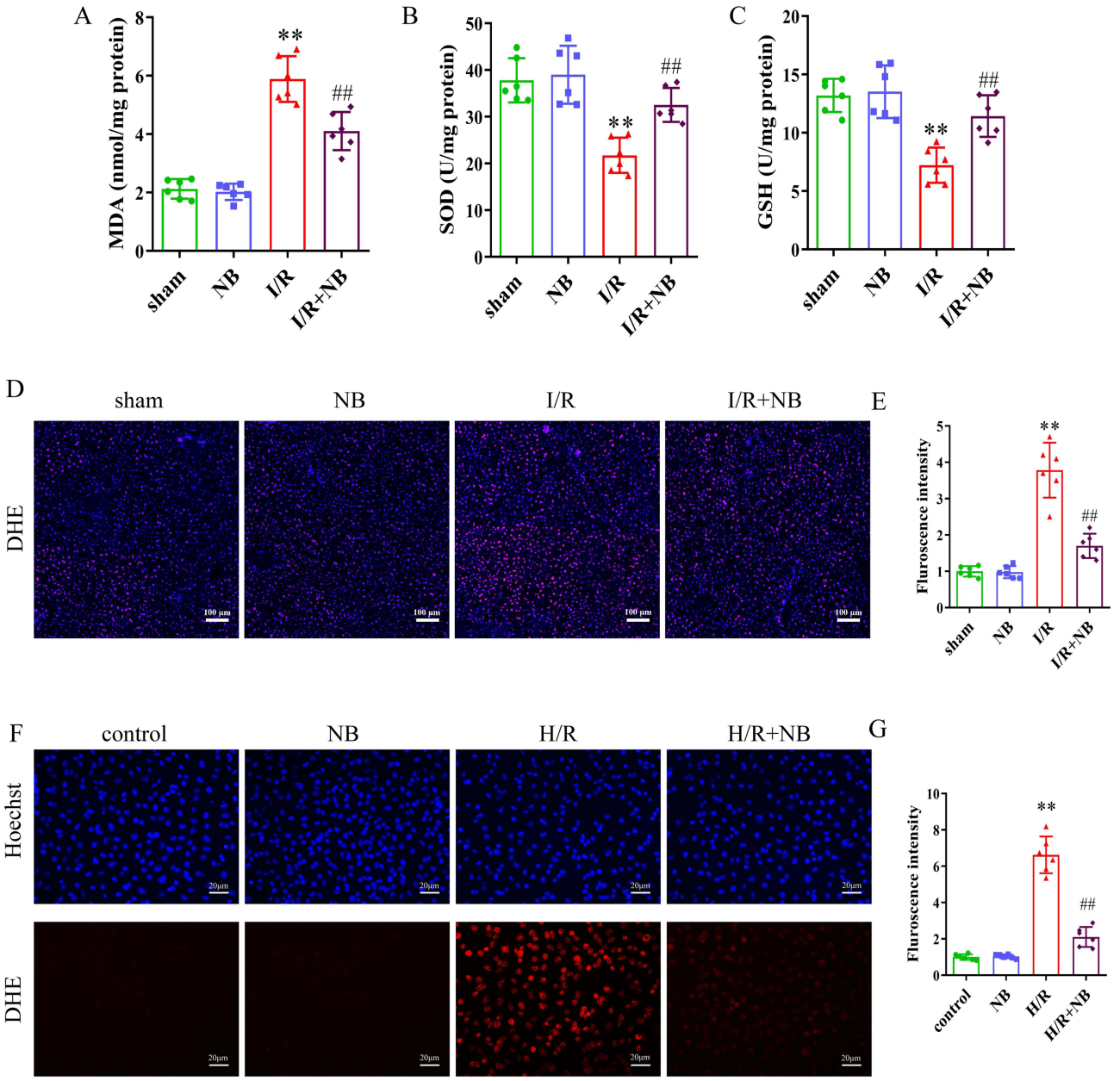

Figure 2 Nepetoidin B alleviates I/R-induced oxidation in vivo and in vitro. (**A**) MDA levels in liver tissue (n = 6/group). (**B**) SOD activity in liver tissue (n = 6/group). (**C**) GSH activity in liver tissue (n = 6/group). (**D**) DHE staining (red fluorescence indicates positive DHE staining) and (**E**) fluorescence intensity analysis of the liver tissue (n = 6/group). (**F**) DHE staining (red fluorescence indicates positive DHE staining) and (**G**) fluorescence intensity analysis of the AML12 cells (n = 6/group). **P < 0.01 vs sham or control group; ##P < 0.01 vs I/R or H/R group.

Nepetoidin B Inhibits JNK/P38 Signaling in vivo and in vitro

To detect changes in the JNK/P38 pathway, we examined changes in JNK/P38 protein phosphorylation in mice and cells. Compared to the sham and control groups, the liver tissue after I/R injury and AML12 cells after H/R injury showed a significant increase in the phosphorylation of JNK and P38 (Figure 5A–F). However, pretreatment with NB significantly reduced the phosphorylation of P38 and JNK after liver I/R and H/R injury (Figure 5A–F). These results suggest that NB pretreatment reduces JNK/P38 activation both in vitro and in vivo.

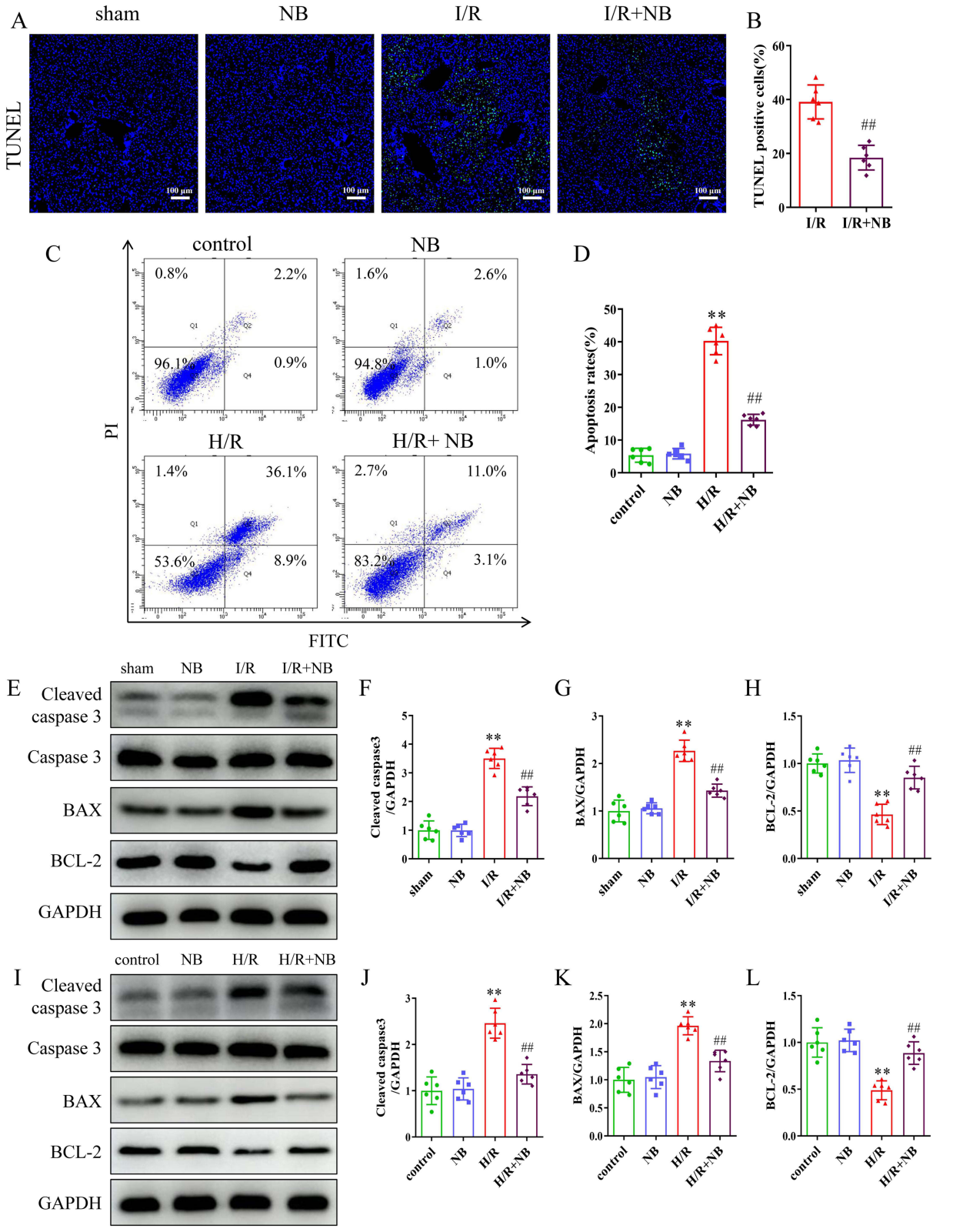

Figure 3 Nepetoidin B alleviates I/R-induced apoptosis in vivo and in vitro. (**A**) TUNEL staining (green fluorescence indicates TUNEL positives cells) and (**B**) statistical analysis of the mouse liver tissue (n = 6/group). (**C** and **D**) Apoptosis was determined using flow cytometry (n = 6/group). (**E**) Detection of apoptotic proteins and (**F–H**) statistical analysis of the mouse liver tissue (n = 6/group). (**I**) Detection of apoptotic proteins and (**J–L**) statistical analysis of the AML12 cells (n = 6/group). **P < 0.01 vs sham or control group; ##P < 0.01 vs I/R or H/R group.

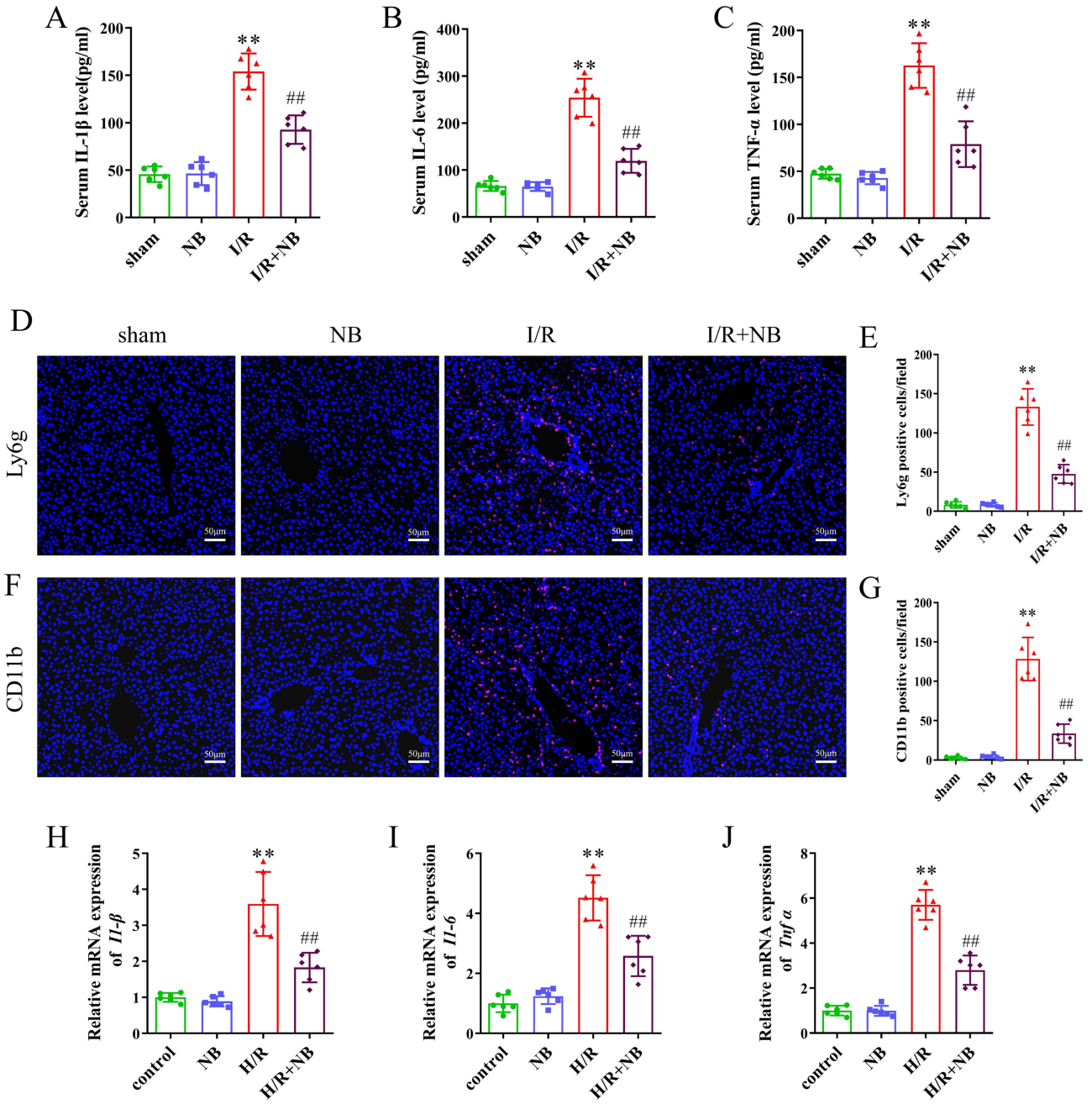

Figure 4 Nepetoidin B alleviates I/R-induced inflammation in vivo and in vitro. (**A**–**C**) Serum contents of IL-1β, IL-6, and TNF-α were detected by ELISA (n = 6/group). (**D**) Ly6g immunofluorescence staining (red fluorescence indicates Ly6g positive cells) and (**E**) statistical analysis of mouse liver tissue (n = 6/group). (**F**) CD11b immunofluorescence staining (red fluorescence indicates CD11b positive cells) and (**G**) statistical analysis of the mouse liver tissue (n = 6/group). (**H**–**J**) mRNA expression of *Il-1β*, *Il-6* and *Tnf-α* in AML12 cells (n = 6/group). **P < 0.01 vs sham or control group; ##P < 0.01 vs I/R or H/R group.

Nepetoidin B Promotes Expression of MKP5 in vivo and in vitro

NB exerts anti-inflammatory effects in RAW 264.7 macrophages by promoting the expression of MKP5. To investigate the potential regulatory role of NB on MKP5 in liver I/R injury, molecular docking of NB with MKP5 was performed. Docking results showed that NB formed salt-bridge hydrogen-bonding interactions with amino acid residues LYS186, SER187, LYS278, GLU183, and Pi-anion interactions with amino acid residues ARG179 and GLU239 of MKP5 with a docking binding energy of −6.0 kcal/mol, which suggests that NB can bind MKP5 more spontaneously (Figure 6A). Furthermore, the protein expression of MKP5 was significantly reduced in the liver tissue after I/R injury and in AML12

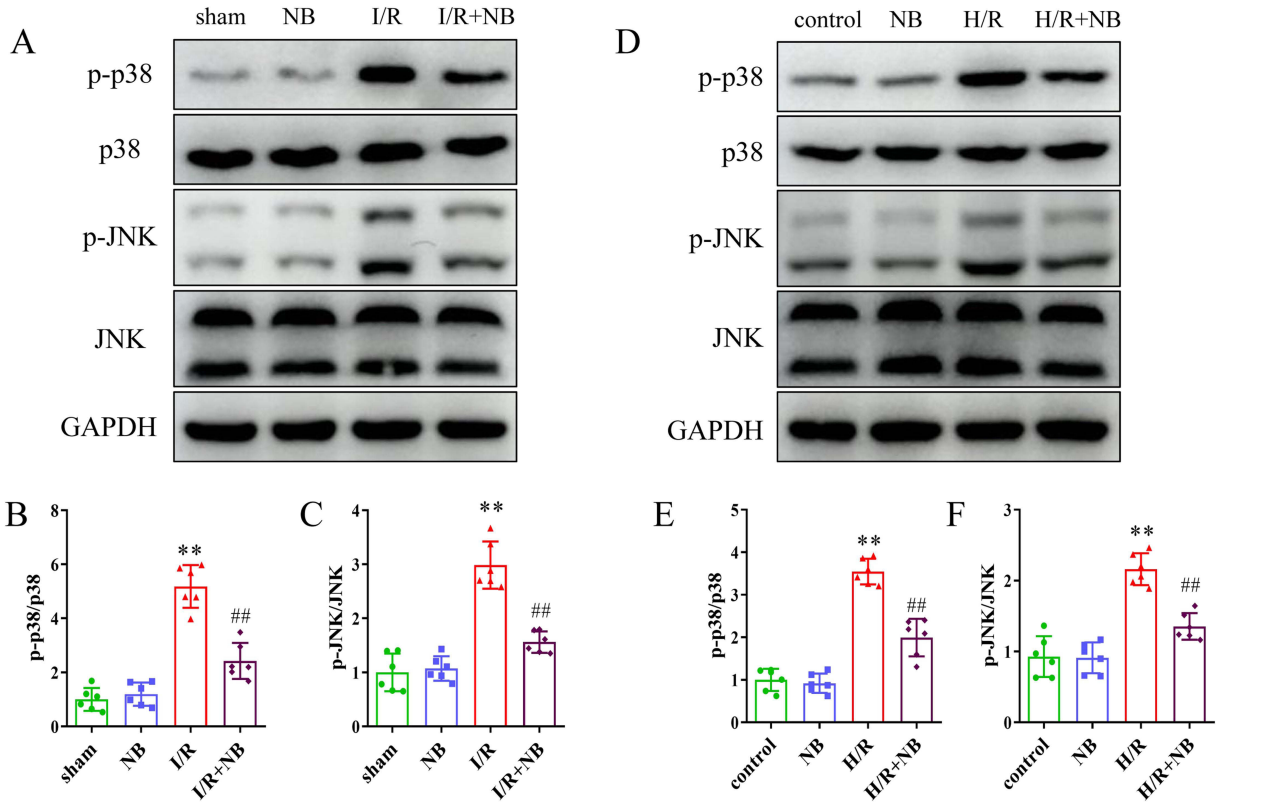

Figure 5 Nepetoidin B inhibits P38/JNK signaling in vivo and in vitro. (**A**) Detection of total and phosphorylated JNK and P38 proteins and (**B** and **C**) statistical analysis of mouse liver tissue (n = 6/group). (**D**) Detection of total and phosphorylated JNK and P38 proteins and (**E** and **F**) statistical analysis of AML12 cells (n = 6/group). **P < 0.01 vs sham or control group; ##P < 0.01 vs I/R or H/R group.

cells after H/R injury (Figure 6B–E). However, pretreatment with NB effectively reversed this decrease in MKP5 expression (Figure 6B–E). These results suggest that NB pretreatment had a positive effect on the expression of MKP5, counteracting the downregulation induced by liver I/R and H/R injury.

MKP5 KO Attenuates Hepatoprotective Effect of Nepetoidin B

To further investigate how NB protects against liver I/R injury, we used MKP5 KO mice to investigate the mechanistic processes involved. Compared to wild-type (WT) mice after I/R injury, ALT and AST levels (Figure 7A and B), liver necrosis area (Figure 7C and D), DHE fluorescence intensity (Figure 7E and F), hepatocyte apoptosis (Figure 7G and H), and inflammatory factors (Figure 7I–K) were significantly increased, and P38/JNK protein phosphorylation was more pronounced after MKP5 KO (Figure 7L and M), suggesting that MKP5 KO aggravated liver I/R injury. Compared to the I/R group, treatment with NB significantly reduced liver injury, oxidative stress, apoptosis, and inflammation following I/R injury (Figure 7A–M). However, liver protection and inhibition of JNK/P38 by NB were significantly diminished in MKP5 KO mice (Figure 7A–M). These results indicate that the protective effects of NB were attenuated by MKP5 KO and that the hepatoprotective effects of NB were associated with the promotion of MKP5 expression.

Discussion

This study explored the potential role of NB in liver I/R injury using a mouse liver I/R injury model and an AML12 H/R cell model. The results showed that NB inhibited liver injury, oxidation, apoptosis, and inflammation; increased cellular activity; and inhibited JNK/P38 protein phosphorylation after liver I/R or cellular H/R injury. In addition, the protective effects of NB were associated with MKP5 expression, whereas its hepatoprotective effects and inhibition of the p38/JNK pathway were substantially diminished after MKP5 KO. Therefore, our results suggest that NB regulates MKP5-mediated P38/JNK signaling to attenuate liver I/R injury by inhibiting oxidative stress, apoptosis, and inflammation (Figure 8).

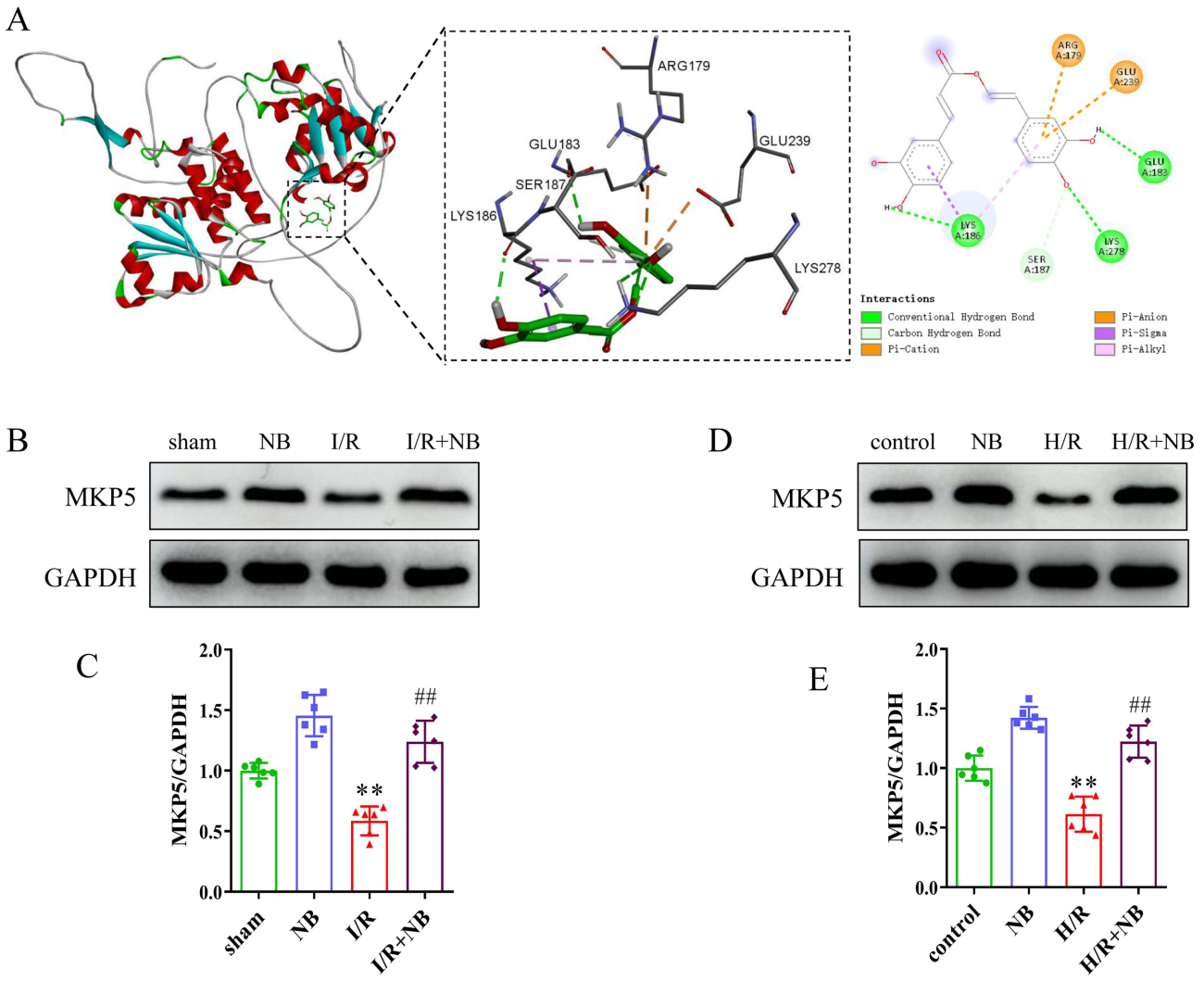

Figure 6 Nepetoidin B promoted the expression of MKP5 in vivo and in vitro. (**A**) Molecular docking of nepetoidin B and MKP5, (**B**) protein detection and (**C**) statistical analysis of MKP5 in mouse liver tissue (n = 6/group). (**D**) Protein detection and (**E**) statistical analysis of MKP5 expression in AML12 cells (n = 6/group). **P < 0.01 vs sham or control group; ##P < 0.01 vs I/R or H/R group.

Restoration of blood flow to the liver after ischemia produces a large concentration of oxygen-free radicals and ROS, which can damage cells.[17] GSH is the key enzyme in the oxygen-free radical scavenging process; it has an obvious scavenging effect on superoxide anions, is a stable metabolite of lipid peroxidation, and is sensitive to oxidative damage caused by oxygen-free radicals.[18,19] DHE staining is a valuable method for visualizing and quantifying the ROS content.[20] GSH, SOD, MDA, and ROS are important indices for assessing oxidative stress during liver I/R injury.[21] MDA and ROS levels in the liver tissue increased significantly following liver I/R injury compared to those in the sham group. In contrast, after NB pretreatment, the MDA and ROS levels were significantly reduced, whereas SOD and GSH levels were significantly increased. The results of liver tissue and DHE staining indicated that NB inhibited oxidation induced by I/R and H/R injury.

Studies have indicated that liver I/R injury is characterized by an increase in inflammatory factors and apoptosis.[22] The liver defense against I/R-induced damage can be achieved by inhibiting inflammatory and apoptosis-related signaling. Liu et al showed that cordycepin attenuates liver I/R injury by inhibiting apoptosis and inflammatory responses.[23] Sun et al showed that lncRNA MALAT1 increases apoptosis and the inflammatory response to aggravate liver I/R injury.[24] In the present study, we examined the serum levels of inflammatory factors IL-1β, IL-6, and TNF-α, and the results showed that NB pretreatment significantly reduced the expression of these inflammatory factors. In

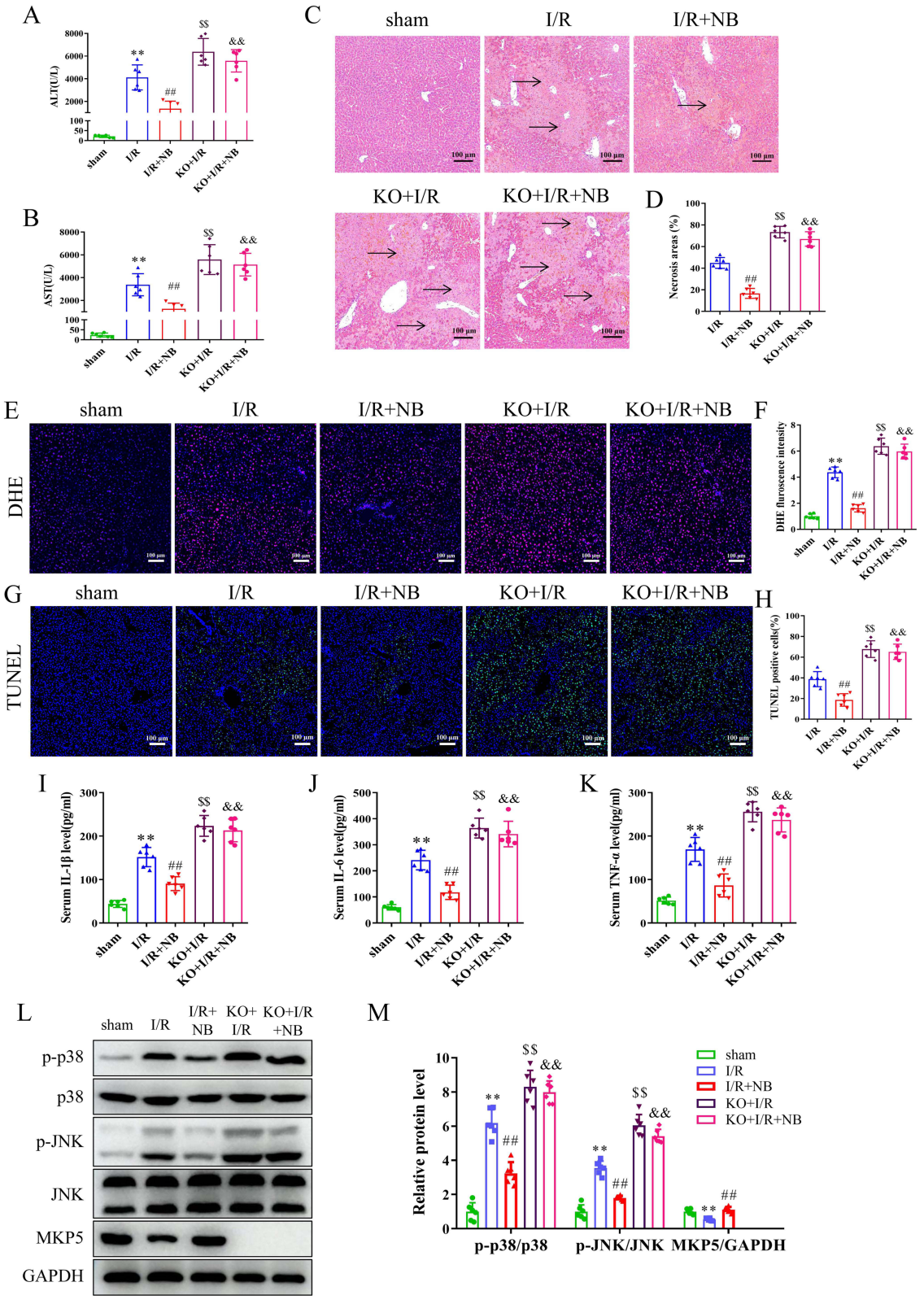

Figure 7 Knockout of MKP5 attenuated the hepatoprotective effect of nepetoidin B. (**A** and **B**) Serum ALT and AST levels (n = 6/group), (**C**) HE staining (the area indicated by the black arrow indicates the necrotic area) and (**D**) necrotic area statistics (n = 6/group), (**E**) DHE staining (red fluorescence indicates positive DHE staining) and (**F**) fluorescence intensity analysis of liver tissue (n = 6/group), (**G**) TUNEL staining (green fluorescence indicates TUNEL-positive cells) and (**H**) statistical analysis (n = 6/group), (**I–K**) serum levels of Il-1β, Il-6, and TNF-α (n = 6/group), (**L** and **M**) protein expression of MKP5, the JNK/P38 pathway, and statistical analysis of liver tissues (n = 6/group). **P < 0.01 vs sham group; ##P < 0.01 vs I/R group; $$P < 0.01 vs I/R group; &&P < 0.01 vs I/R+NB group.

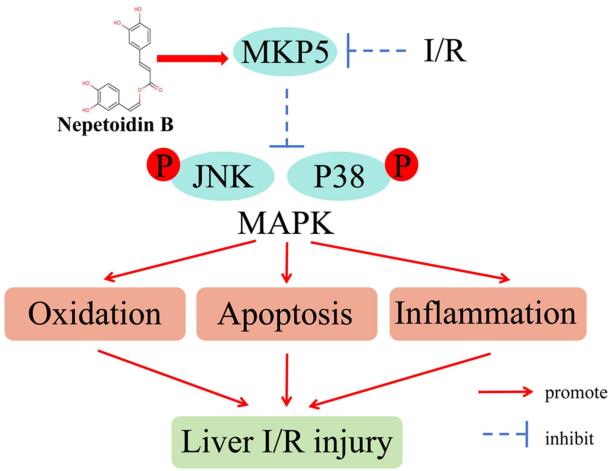

Figure 8 The schematic representation of the mechanism by which nepetoidin B alleviates liver ischemia/reperfusion injury.

addition, immunofluorescence staining indicated that NB pretreatment significantly reduced the infiltration of $Ly6g^+$ and $CD11b^+$ cells. The measurement of *Il-1β, Il-6*, and *Tnf*-α mRNA expression also indicated that NB inhibited H/R-induced inflammatory response. Moreover, TUNEL staining showed that NB pretreatment significantly reduced apoptosis. The anti-apoptotic effects of NB in the liver and AML12 cells were further confirmed using apoptosis-associated proteins. Therefore, our findings suggested that NB inhibited apoptosis and inflammatory responses in I/R-injured liver.

MAPK plays an important role in membrane receptor signal transduction and regulates numerous cellular processes, including cell growth, migration, differentiation, and inflammation.[25] The MAPK family includes ERK, JNK, and the P38MAPK pathway.[26] The MAPK family plays a key role in mediating I/R injury in the liver and regulating hepatocyte death and survival by regulating signaling pathways related to oxidative stress, apoptosis and inflammatory responses.[11] For example, the six-transmembrane epithelial antigen of the prostate 3 attenuates liver I/R injury by inhibiting the TAK1-mediated JNK/p38 signaling pathway.[27] N-acetylgalactosaminyltransferase-4 protects against liver I/R injury by inhibiting the ASK1-JNK/p38 pathway.[28] In the current study, we observed the activation of the P38/JNK signaling pathway in mouse livers following I/R injury and in AML12 cells subjected to H/R injury, as evidenced by the increased phosphorylation levels of P38 and JNK. However, NB pretreatment significantly inhibited the activation of the JNK/p38 pathway in mouse livers injured by I/R and in AML12 cells damaged by H/R.

MKP5 belongs to the MKP family, which inactivates target kinases by dephosphorylating phosphoserine/threonine and phosphotyrosine residues.[14] As a negative regulator of the MAPK signaling pathway, MKP5 is closely associated with many diseases.[13] For example, MKP5 can limit P38 and JNK activation and attenuate lipopolysaccharide (LPS)-induced vascular injury.[29] MKP5 KO in mice increased the activation of the MAPK signaling pathway, thus exacerbating LPS-induced lung injury.[30] Previous studies have shown that NB inhibits LPS-stimulated NO production by promoting MKP5 expression in RAW 264.7 macrophages.[10] To explore the regulatory effects of NB on MKP5, we docked NB with MKP5 using molecular docking. NB was able to effectively bind to MKP5 with a binding energy of −6.0 kcal/mol, indicating that NB is able to bind MKP5 more spontaneously.[31] In addition, NB promoted the expression of MKP5 in the liver tissue and AML12 cells. To investigate whether the hepatoprotective effect of NB was mediated by the promotion of MKP5 expression, we verified this in MKP5 KO mice. Consistent with our previous research, activation of the JNK/p38 pathway was more pronounced, liver damage was more severe after MKP5 KO,[32] and the protective effects of NB were significantly reduced in MKP5 KO mice.

This study is the first to demonstrate that NB protects the liver from I/R injury and that regulates the MKP5-mediated JNK/P38 pathway. However, this study had some limitations. Given that there are only a few studies on NB, more experiments are needed to explore the optimal dose and timing of NB administration. The present study explored the anti-oxidative, anti-apoptotic, and anti-inflammatory effects of NB on the P38/JNK signaling pathway. However, it remains unclear whether NB ameliorates liver I/R injury by regulating other signaling pathways, and the direct regulatory relationship between NB and MKP5 requires further investigation. We hope that our future research addresses these questions.

Conclusion

In conclusion, pretreatment with NB attenuates I/R injury in the liver by inhibiting oxidative stress, apoptosis, and inflammation. This protective mechanism may be associated with the promotion of MKP5 expression, which in turn inhibits the activation of the P38/JNK signaling pathway. These findings will provide new insights into research on potent therapeutics to treat and prevent liver I/R injury.

Data Sharing Statement

The data underlying this article will be shared upon reasonable request by the corresponding author.

Acknowledgments

We thank Professor Yinming Liang from Xinxiang Medical College for providing the MKP5 knockout mice.

Author Contributions

All authors made a significant contribution to the work reported, whether in the conception, study design, execution, acquisition of data, analysis, and interpretation, or in all these areas, took part in drafting, revising, or critically reviewing the article; gave final approval of the version to be published; have agreed on the journal to which the article has been submitted; and agree to be accountable for all aspects of the work.

Funding

This study was supported by the National Natural Science Foundation of China (grant no. 82201963).

Disclosure

The authors declare no conflicts of interest regarding the publication of this article.

References

1. Saidi R, Kenari S. Liver ischemia/reperfusion injury: an overview. *J Invest Surg*. 2014;27(6):366–379. doi:10.3109/08941939.2014.932473
2. Nastos C, Kalimeris K, Papoutsidakis N, et al. Global consequences of liver ischemia/reperfusion injury. *Oxid Med Cell Longev*. 2014;2014:906965. doi:10.1155/2014/906965
3. Quesnelle K, Bystrom P, Toledo-Pereyra L. Molecular responses to ischemia and reperfusion in the liver. *Arch Toxicol*. 2015;89(5):651–657. doi:10.1007/s00204-014-1437-x
4. Liu J, Man K. Mechanistic insight and clinical implications of ischemia/reperfusion injury post liver transplantation. *Cell Mol Gastroenter*. 2023;15(6):1463–1474. doi:10.1016/j.jcmgh.2023.03.003
5. Nakazato P, Victorino J, Fina C, et al. Liver ischemia and reperfusion injury. Pathophysiology and new horizons in preconditioning and therapy. *Acta Cir Bras*. 2018;33(8):723–735. doi:10.1590/s0102-865020180080000008
6. Marinho H, Marcelino P, Soares H, Corvo M. Gene silencing using siRNA for preventing liver ischaemia-reperfusion injury. *Curr Pharm Design*. 2018;24(23):2692–2700. doi:10.2174/1381612824666180807124356
7. Dossi C, Vargas R, Valenzuela R, Videla L. Beneficial effects of natural compounds on experimental liver ischemia-reperfusion injury. *Food Funct*. 2021;12(9):3787–3798. doi:10.1039/d1fo00289a
8. Grayer R, Eckert M, Veitch N, et al. The chemotaxonomic significance of two bioactive caffeic acid esters, nepetoidins A and B, in the Lamiaceae. *Phytochemistry*. 2003;64(2):519–528. doi:10.1016/s0031-9422(03)00192-4
9. Kim M, Kim J, Yang H, Choe J, Hwang I. Salvia plebeia Nepetoidin B from R. Br. inhibits inflammation by modulating the NF-κB and Nrf2/HO-1 signaling pathways in macrophage cells. *Antioxidants-Basel*. 2021;10(8). doi:10.3390/antiox10081208
10. Wu X, Gao H, Sun W, et al. Nepetoidin B, a natural product, inhibits LPS-stimulated nitric oxide production via modulation of iNOS mediated by NF-κB/MKP-5 pathways. *Phytother Res*. 2017;31(7):1072–1077. doi:10.1002/ptr.5828
11. Yu B, Zhang Y, Wang T, et al. MAPK signaling pathways in hepatic ischemia/reperfusion injury. *J Inflamm Res*. 2023;16:1405–1418. doi:10.2147/JIR.S396604
12. Bi J, Zhang J, Ke M, et al. HSF2BP protects against acute liver injury by regulating HSF2/HSP70/MAPK signaling in mice. *Cell Death Dis*. 2022;13(9):830. doi:10.1038/s41419-022-05282-x
13. Jiménez-Martínez M, Stamatakis K, Fresno M. The Dual-Specificity Phosphatase 10 (DUSP10): its role in cancer, inflammation, and immunity. *Int J Mol Sci*. 2019;20(7):1626. doi:10.3390/ijms20071626
14. Theodosiou A, Smith A, Gillieron C, Arkinstall S, Ashworth A. MKP5, a new member of the MAP kinase phosphatase family, which selectively dephosphorylates stress-activated kinases. *Oncogene*. 1999;18(50):6981–6988. doi:10.1038/sj.onc.1203185
15. Zhang J, Zhang M, Zhang J, Xia Q. A novel mouse model of liver ischemic/reperfusion injury and its differences to the existing model. *J Invest Surg*. 2015;28(5):283–291. doi:10.3109/08941939.2014.983621
16. Yu Q, Chen S, Tang H, et al. Veratric acid alleviates liver ischemia/reperfusion injury by activating the Nrf2 signaling pathway. *Int Immunopharmacol*. 2021;101:108294. doi:10.1016/j.intimp.2021.108294

17. Serrano E, Diaz J, Acosta F, Palenciano C, Parrilla P, Carbonell L. Oxidative stress during ischemia-reperfusion in liver transplantation. *Transpl P*. 2000;32(8):2651. doi:10.1016/s0041-1345(00)01824-8
18. Shen Y, Shen X, Cheng Y, Liu Y. Myricitrin pretreatment ameliorates mouse liver ischemia reperfusion injury. *Int Immunopharmacol*. 2020;89:107005. doi:10.1016/j.intimp.2020.107005
19. Ye J, Peng J, Liu K, Zhang T, Huang W. MCTR1 inhibits ferroptosis by promoting NRF2 expression to attenuate hepatic ischemia-reperfusion injury. *Am J Physiol Gastr Liver Physiol*. 2022;323(3):G283–G293. doi:10.1152/ajpgi.00354.2021
20. Fernandes D, Gonçalves R, Laurindo F. Measurement of superoxide production and NADPH oxidase activity by HPLC analysis of dihydroethidium oxidation. *Methods Mol Biol*. 2017;1527:233–249. doi:10.1007/978-1-4939-6625-7_19
21. Li J, Li J, Fang H, et al. Isolongifolene alleviates liver ischemia/reperfusion injury by regulating AMPK-PGC1α signaling pathway-mediated inflammation, apoptosis, and oxidative stress. *Int Immunopharmacol*. 2022;113:109185. doi:10.1016/j.intimp.2022.109185
22. Kahan R, Cray P, Abraham N, et al. Sterile inflammation in liver transplantation. *Front Med Lausanne*. 2023;10:1223224. doi:10.3389/fmed.2023.1223224
23. Liu Y, Sheng M, Jia L, Zhu M, Yu W. Protective effects of cordycepin pretreatment against liver ischemia/reperfusion injury in mice. *Immun Inflamm Dis*. 2023;11(3):e792. doi:10.1002/iid3.792
24. Sun Q, Gong J, Gong X, et al. Long non-coding RNA MALAT1 aggravated liver ischemia-reperfusion injury via targeting miR-150-5p/AZIN1. *Bioengineered*. 2022;13(5):13422–13436. doi:10.1080/21655979.2022.2073124
25. Kim E, Choi E. Compromised MAPK signaling in human diseases: an update. *Arch Toxicol*. 2015;89(6):867–882. doi:10.1007/s00204-015-1472-2
26. Liang Y, Yang W. Kinesins in MAPK cascade: how kinesin motors are involved in the MAPK pathway? *Gene*. 2019;684:1–9. doi:10.1016/j.gene.2018.10.042
27. Guo W, Fang H, Cao S, et al. Six-transmembrane epithelial antigen of the prostate 3 deficiency in hepatocytes protects the liver against ischemia-reperfusion injury by suppressing transforming growth factor-β-activated kinase 1. *Hepatology*. 2020;71(3):1037–1054. doi:10.1002/hep.30882
28. Zhou J, Guo L, Ma T, et al. N-acetylgalactosaminyltransferase-4 protects against hepatic ischemia/reperfusion injury by blocking apoptosis signal-regulating kinase 1 N-terminal dimerization. *Hepatology*. 2022;75(6):1446–1460. doi:10.1002/hep.32202
29. Qian F, Deng J, Cheng N, et al. A non-redundant role for MKP5 in limiting ROS production and preventing LPS-induced vascular injury. *EMBO J*. 2009;28(19):2896–2907. doi:10.1038/emboj.2009.234
30. Qian F, Deng J, Gantner B, et al. Map kinase phosphatase 5 protects against sepsis-induced acute lung injury. *Am J Physiol-Lung C*. 2012;302(9):L866–L874. doi:10.1152/ajplung.00277.2011
31. Pinzi L, Rastelli G. Molecular docking: shifting paradigms in drug discovery. *Int J Mol Sci*. 2019;20(18). doi:10.3390/ijms20184331
32. Yu Q, Chen S, Li J, et al. Mitogen activated protein kinase phosphatase 5 alleviates liver ischemia-reperfusion injury by inhibiting TAK1/JNK/p38 pathway. *Sci Rep*. 2023;13(1):11110. doi:10.1038/s41598-023-37768-9